SURFACE COMPOSITIONS ON PLUTO AND CHARON. W.M. Grundy,[1] R.P. Binzel,[2] J.C. Cook,[3] D.P. Cruikshank,[4] C.M. Dalle Ore,[5,4] A.M. Earle,[2] K. Ennico,[4] D.E. Jennings,[6] C.J.A. Howett,[3] I.R. Linscott, A.W. Lunsford,[6] C.B. Olkin,[3] A.H. Parker,[3] J.Wm. Parker,[3] S. Philippe,[7] S. Protopapa,[8] E. Quirico[7], D.C. Reuter,[6] B. Schmitt,[7] K.N. Singer,[3] J.R. Spencer,[3] J.A. Stansberry,[9] S.A. Stern,[3] C.C.C. Tsang,[3] A.J. Verbiscer,[10] H.A. Weaver,[11] L.A. Young[3], K.L. Berry[12,13], B.J. Buratti[14], and the New Horizons Science Team. [1]Lowell Observatory, Flagstaff AZ (w.grundy@lowell.edu), [2]Massachusetts Institute of Technology, [3]Southwest Research Institute, [4]NASA Ames Research Center, [5]SETI Institute, [6]NASA Goddard Space Flight Center, [7]Université Grenoble Alpes / CNRS - IPAG, [8]University of Maryland, [9]Space Telescope Science Institute, [10]University of Virginia, [11]Johns Hopkins University Applied Physics Laboratory, [12]Northern Arizona University, [13]United States Geological Survey, [14]NASA Jet Propulsion Laboratory.

Introduction: After nearly a decade en route, New Horizons flew through the Pluto system in July 2015. The spacecraft's sophisticated suite of instruments revealed a spectacularly complex system [1]. This presentation focuses on the surface compositions of the two largest bodies, Pluto and Charon.

New Horizons' primary instrument for mapping surface compositions is Ralph, a near-infrared spectral imager paired with a CCD camera system [2]. Ralph's Linear Etalon Imaging Spectral Array (LEISA) component provides spectral coverage from 1.25 – 2.5 μm, at a resolving power (λ/Δλ) of 240. The Multi-spectral Visible Imaging Camera (MVIC) includes 4 CCD arrays with affixed interference filters covering wavelengths from “BLUE” (400-550 nm), through “RED” (540-700 nm), “NIR” (780-975 nm), and a methane absorption band “CH4” (860-910 nm). Ralph normally operates in a scanning mode with the spacecraft sweeping its field of view across the scene, to accumulate the data needed to assemble a multi-wavelength image.

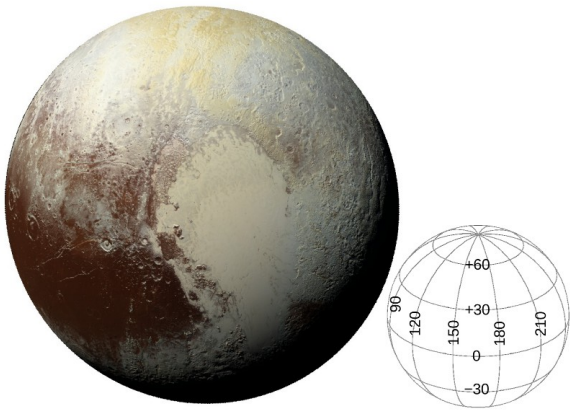

Fig. 1. “Enhanced” color view of Pluto's encounter hemisphere with MVIC BLUE, RED, and NIR filters displayed in blue, green, and red channels, respectively. A full resolution version is available at www.nasa.gov/newhorizons.

Pluto: MVIC color imaging of Pluto's encounter hemisphere (the anti-Charon hemisphere) at 700 m/pixel resolution reveals a latitude-dependent distribution of colors (Fig. 1). An equatorial belt of dark, heavily-cratered, reddish terrain exemplified by Cthulhu Regio[1] gives way to lighter reddish terrains that grade into a neutral mid-latitude belt and finally golden hues at the pole (Lowell Regio). This latitudinal pattern is dramatically interrupted by the bright, heart-shaped Tombaugh Regio (TR).

LEISA spectral imaging of Pluto at 6 to 7 km/pixel resolution reveals the encounter hemisphere to be dominated by volatile ices of N_2, CO, and CH_4, along with non-volatile (at least at Pluto temperatures) components including H_2O and tholins [3]. The spatial distributions of these materials (Fig. 2) are highly revealing. The most volatile of Pluto's ices (N_2 and CO) are especially prevalent in the western half of TR, the strikingly flat Sputnik Planum (SP). SP occupies a large basin-like feature a few km below surrounding elevations. The high mobility of N_2 and CO ices enables SP's surface to refresh itself sufficiently rapidly that no impact craters are seen there [4]. This likely occurs through a combination of solid state convective overturning (as

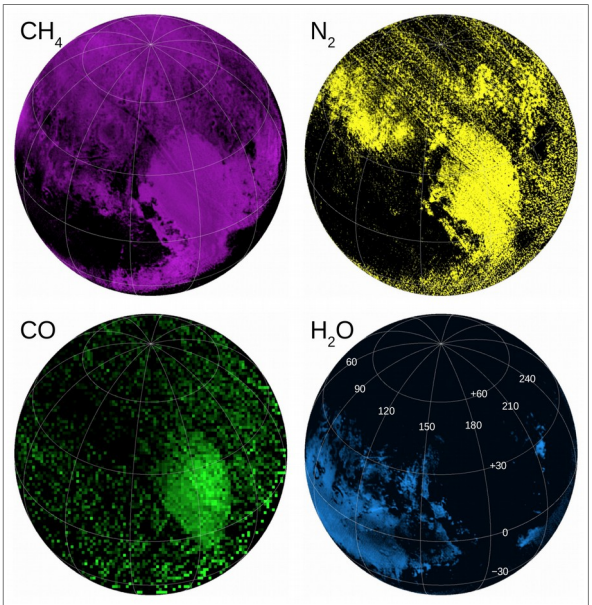

Fig. 2. Pluto compositional maps indicating regions rich in ices of CH_4, N_2, CO, and H_2O.

1 All place names throughout this abstract and the associated talk are informal.

evidenced by the presence of cellular patterns on a scale of tens of km) and sublimation/ condensation (as evidenced by regular patterns of pits and ridges on scales of 10^2 to 10^3 m). N_2 ice also appears in mid-latitude topographic lows, such as the floors of craters.

CH_4 ice is less volatile than N_2 and CO ices at Pluto surface temperatures, but it is still mobile. CH_4 occurs on SP, but it is also seen in other regions where N_2 and CO absorptions are less evident, including the northern polar region, the eastern half of TR, and along the periphery of the dark, red, equatorial terrains. In many areas, CH_4 appears to favor topographically high regions. Its propensity to condense on ridges could play an important role in constructing the bizarre bladed terrain seen in Tartarus Dorsa.

The characteristic absorptions of non-volatile H_2O ice are most evident at latitudes below about 30° (except for TR). H_2O can be discerned across much of Cthulhu Regio, and also in a few isolated spots, such as Virgil Fossa and Viking Terra. In many of these regions, H_2O absorption is associated with reddish tholin coloration. Since both are inert, H_2O ice and tholin could have similar geological behaviors on Pluto, possibly including aeolian transport or mobilization by volatile ice glaciation. But in another isolated H_2O-rich region around Pulfrich crater, the reddish coloration is lacking, so the two materials are not always associated.

For structural integrity, rugged mountains like al-Idrisi and Zheng-He should be composed of H_2O ice [1], but they show relatively weak H_2O spectral signatures. Evidently their H_2O is partially hidden beneath a veneer of more volatile ices. Geochemically, H_2O should be ubiquitous. It likely makes up the bulk of Pluto's mantle [5]. Although H_2O should be geologically inert at such low temperatures, it is clearly participating in Pluto's active geology, appently enabled by the action of the more volatile ices on it.

Charon: Whereas Pluto's H_2O ice is sculpted and at least partially veiled by more volatile ices, Charon's heavily cratered H_2O ice is exposed for all to see (Fig. 3). H_2O ice bands at 1.5, 1.65, and 2 μm, which are characteristic of cold, crystalline ice, are seen everywhere on Charon's encounter hemisphere. But despite being ubiquitously coated in H_2O ice, the same material that dominates the surfaces of numerous comparably-sized satellites of Saturn and Uranus, Charon manages to be unique among icy satellites.

Charon's north polar region is strikingly red. This area, Mordor Macula, is likely the result of the unique thermal environment of Charon's poles, which become exceptionally cold during the long, dark winters. Extremely low temperatures enable volatiles such as CH_4 that would not otherwise be stable on Charon's surface

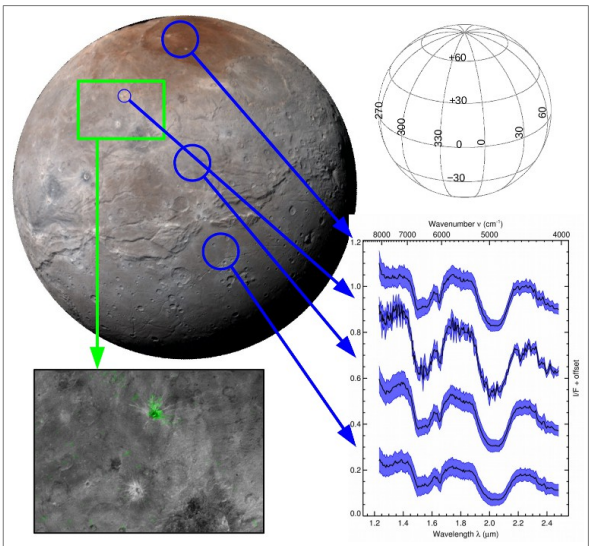

Fig. 3. "Enhanced" color view of Charon's encounter hemisphere showing the reddish pole. A full resolution version is available at www.nasa.gov/newhorizons. LEISA spectra extracted in various regions are plotted in blue. All are dominated by the characteristic features of cold, crystalline H_2O ice. In Organa crater, NH_3 absorption is seen at around 2.22 μm. That absorption band is mapped in green in the inset at lower left.

to become temporarily cold trapped as ices. Frozen CH_4 can be very rapidly radiolytically processed *in situ* into heavier and less volatile molecules that are precursors to tholins [3,6].

Charon also exhibits a weak NH_3 absorption at about 2.22 μm, as known from Earth-based observations [7,8,9,10]. This absorption band is seen to be strongest in a few isolated regions, most strikingly Organa crater. It is possible that this particular crater is too young for NH_3 excavated from Charon's subsurface to have been radiolytically destroyed (estimated to occur in ~10^7 years [9]). Other ideas include Charon's subsurface having local concentrations of NH_3 thanks to a history of cryovolcanism, or that the NH_3 was delivered by an impactor, or is created by processing of local N-bearing precursor materials [11].

References: [1] Stern et al. (2015) Science, 350, 292. [2] Reuter et al. (2008) SSR, 140, 129-154. [3] Grundy et al. (2016) Science, submitted. [4] Moore et al. (2016) Science, submitted. [5] McKinnon & Mueller (1988) Nature 335, 240-243. [6] Tucker et al. (2015) Icarus 246, 291-297. [7] Brown & Calvin (2000) Science 287, 107-109. [8] Buie & Grundy (2000) Icarus 148, 324-339. [9] Cook et al. (2007) ApJ. 663, 1406-1419. [10] de Meo et al. (2015) Icarus 246, 213-219. [11] Cruikshank et al. (this meeting).